CHAPTER 4

TWO-PHASE FLOW

TWO-PHASE FLOW is encountered extensively in the air-conditioning, heating, and refrigeration industries. A combination of liquid and vapor refrigerant exists in flooded coolers, direct-expansion coolers, thermosiphon coolers, brazed and gasketed plate evaporators and condensers, and tube-in-tube evaporators and condensers, as well as in air-cooled evaporators and condensers. In the pipes of heating systems, steam and liquid water may both be present. Because the hydrodynststamic and heat transfer aspects of two-phase flow are not as well understood as those of single-phase flow, no single set of correlations can be used to predict pressure drops or heat transfer rates. Instead, the correlations are for specific thermal and hydrodynamic operating conditions.

This chapter presents the basic principles of two-phase flow and provides information on the vast number of correlations that have been developed to predict heat transfer coefficients and pressure drops in these systems.

BOILING

Commonly used refrigeration evaporators are (1) flooded evaporators, where refrigerants at low fluid velocities boil outside or inside tubes; and (2) dry expansion shell-and-tube evaporators, where refrigerants at substantial fluid velocities boil outside or inside tubes.

Two-phase heat and mass transport are characterized by various flow and thermal regimes, whether vaporization takes place under natural convection or in forced flow. Unlike single-phase flow systems, the heat transfer coefficient for a two-phase mixture depends on the flow regime, the thermodynamic and transport properties of both the vapor and the liquid, the roughness of the heating surface, the wetting characteristics of the surface-liquid pair, and other parameters. Therefore, it is necessary to consider each flow and boiling regime separately to determine the heat transfer coefficient.

Accurate data defining limits of regimes and determining the effects of various parameters are not available. The accuracy of correlations in predicting the heat transfer coefficient for two-phase flow is in most cases not known beyond the range of the test data.

Boiling and Pool Boiling in Natural Convection Systems

Regimes of Boiling. The different regimes of pool boiling described by Farber and Scorah (1948) verified those suggested by Nukiyama (1934). The regimes are illustrated in Figure 1. When the temperature of the heating surface is near the fluid saturation temperature, heat is transferred by convection currents to the free surface where evaporation occurs (Region I). Transition to nucleate boiling occurs when the surface temperature exceeds saturation by a few degrees (Region II).

In **nucleate boiling** (Region III), a thin layer of superheated liquid is formed adjacent to the heating surface. In this layer, bubbles nucleate and grow from spots on the surface. The thermal resistance

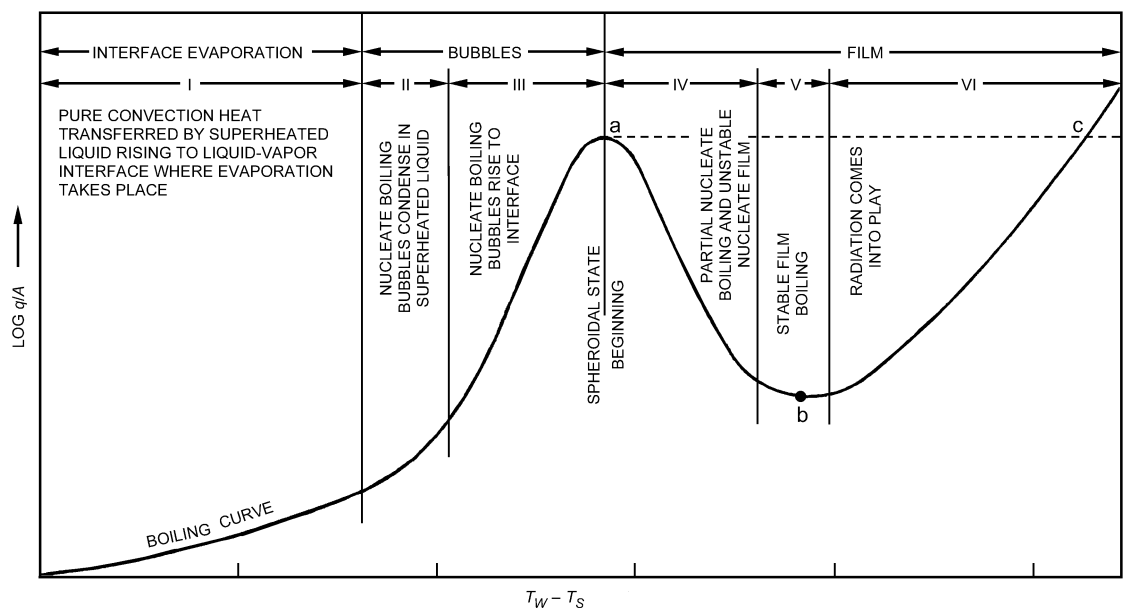

Fig. 1 Characteristic Pool Boiling Curve

The preparation of this chapter is assigned to TC 1.3, Heat Transfer and Fluid Flow.

of the superheated liquid film is greatly reduced by bubble-induced agitation and vaporization. Increased wall temperature increases bubble population, causing a large increase in heat flux.

As heat flux or temperature difference increases further and as more vapor forms, the flow of the liquid toward the surface is interrupted, and a vapor blanket forms. This gives the **maximum heat flux**, which is at the departure from nucleate boiling (DNB) at point a, Figure 1. This flux is often termed the **burnout heat flux** or **boiling crisis** because, for constant power-generating systems, an increase of heat flux beyond this point results in a jump of the heater temperature (to point c, Figure 1), often beyond the melting point of a metal heating surface.

In systems with controllable surface temperature, an increase beyond the temperature for DNB causes a decrease of heat flux density. This is the **transition boiling regime** (Region IV); liquid alternately falls onto the surface and is repulsed by an explosive burst of vapor.

At sufficiently high surface temperatures, a stable vapor film forms at the heater surface; this is the **film boiling regime** (Regions V and VI). Because heat transfer is by conduction (and some radiation) across the vapor film, the heater temperature is much higher than for comparable heat flux densities in the nucleate boiling regime. The minimum film boiling (MFB) heat flux (point b) is the lower end of the film boiling curve.

Free Surface Evaporation. In Region I, where surface temperature exceeds liquid saturation temperature by less than a few degrees, no bubbles form. Evaporation occurs at the free surface by convection of superheated liquid from the heated surface. Correlations of heat transfer coefficients for this region are similar to those for fluids under ordinary natural convection [Equations (1) through (4) in Table 1].

Nucleate Boiling. Much information is available on boiling heat transfer coefficients, but no universally reliable method is available for correlating the data. In the nucleate boiling regime, heat flux density is not a single, valued function of the temperature but depends also on the nucleating characteristics of the surface, as illustrated by Figure 2 (Berenson 1962).

The equations proposed for correlating nucleate boiling data can be put in a form that relates heat transfer coefficient h to temperature difference $(t_w - t_{sat})$:

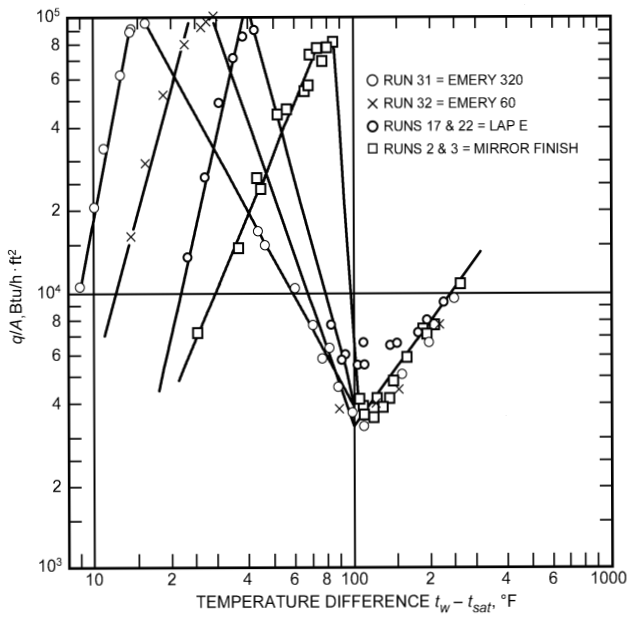

Fig. 2 Effect of Surface Roughness on Temperature in Pool Boiling of Pentane

$$h = \text{constant}\ (t_w - t_{sat})^a \quad (1)$$

Exponent a is normally about 3 for a plain, smooth surface; its value depends on the thermodynamic and transport properties of the vapor and the liquid. Nucleating characteristics of the surface, including the size distribution of surface cavities and the wetting characteristics of the surface-liquid pair, affect the value of the multiplying constant and the value of the exponent a in Equation (1).

A generalized correlation cannot be expected without consideration of the nucleating characteristics of the heating surface. A statistical analysis of data for 25 liquids by Hughmark (1962) shows that in a correlation not considering surface condition, deviations of more than 100% are common.

In the following sections, correlations and nomographs for prediction of nucleate and flow boiling of various refrigerants are given. For most cases, these correlations have been tested for refrigerants, such as R-11, R-12, R-113, and R-114, that have now been identified as environmentally harmful and are no longer being used in new equipment. Extensive research on the thermal and fluid characteristics of alternative refrigerants/refrigerant mixtures has taken place in recent years, and some correlations have been suggested.

Stephan and Abdelsalam (1980) developed a statistical approach for estimating the heat transfer during nucleate boiling. The correlation [Equation (5) in Table 1] should be used with a fixed contact angle θ regardless of the fluid. Cooper (1984) proposed a dimensional correlation for nucleate boiling, shown as Equation (6) in Table 1. The dimensions required are listed in Table 1. This correlation is recommended for fluids with poorly defined physical properties.

Gorenflo (1993) proposed a nucleate boiling correlation based on a set of reference conditions and a base heat transfer coefficient as shown in Equation (7) in Table 1. The correlation was developed for a reduced pressure p_r of 0.1 and the reference conditions given in Table 1. Base heat transfer coefficients are given for three fluids in Table 1, and Gorenflo (1993) should be consulted for additional fluids.

In addition to correlations dependent on thermodynamic and transport properties of the vapor and the liquid, Borishansky et al. (1962) and Lienhard and Schrock (1963) documented a correlating method based on the law of corresponding states. The properties can be expressed in terms of fundamental molecular parameters, leading to scaling criteria based on the reduced pressure, $p_r = p/p_c$, where p_c is the critical thermodynamic pressure for the coolant. An example of this method of correlation is shown in Figure 3. The reference pressure p^* was chosen as $p^* = 0.029p_c$. This correlation provides a simple method for scaling the effect of pressure if data are available for one pressure level. It also has an advantage if the thermodynamic and particularly the transport properties used in several equations in Table 1 are not accurately known. In its present form, this correlation gives a value of $a = 2.33$ for the exponent in Equation (1) and consequently should apply for typical aged metal surfaces.

There are explicit heat transfer coefficient correlations based on the law of corresponding states for various substances (Borishansky and Kosyrev 1966), halogenated refrigerants (Danilova 1965), and flooded evaporators (Starczewski 1965). Other investigations examined the effects of oil on boiling heat transfer from diverse configurations, including boiling from a flat plate (Stephan 1963b); a 0.55 in. OD horizontal tube using an oil-R-12 mixture (Tschernobyiski and Ratiani 1955); inside horizontal tubes using an oil-R-12 mixture (Breber et al. 1980, Worsoe-Schmidt 1959, Green and Furse 1963); and commercial copper tubing using R-11 and R-113 with oil content to 10% (Dougherty and Sauer 1974). Additionally, Furse (1965) examined R-11 and R-12 boiling over a flat horizontal copper surface.

Table 1 Equations for Boiling Heat Transfer

Description	References	Equations
Free convection Free convection boiling, or boiling without bubbles for low Δt and GrPr < 10^8 (all properties based on liquid state)	Jakob (1949 and 1957)	$\mathrm{Nu} = C(\mathrm{Gr})^m(\mathrm{Pr})^n$ (1)
Vertical submerged surface		$\mathrm{Nu} = 0.61(\mathrm{Gr})^{0.25}(\mathrm{Pr})^{0.25}$ (2)
Horizontal submerged surface		$\mathrm{Nu} = 0.16(\mathrm{Gr})^{1/3}(\mathrm{Pr})^{1/3}$ (3)
Simplified equation for water		$h \sim 80(\Delta t)^{1/3}$, where h is in Btu/h·ft²·°F, Δt in °F (4)
Nucleate boiling	Stephan and Abdelsalam (1980)	$\frac{hD_d}{k_L} = 0.0546\left[\left(\frac{\rho_v}{\rho_l}\right)^{0.5}\left(\frac{qD_d}{Ak_lT_{sat}}\right)\right]^{0.67}\left(\frac{h_{fg}D_d^2}{a_L^2}\right)^{0.248}\left(\frac{\rho_l-\rho_v}{\rho_l}\right)^{-4.33}$ (5) where $D_d = 0.0208\theta\left[\frac{\sigma}{g(\rho_l-\rho_v)}\right]^{1/2}$ with $\theta = 35°$
	Cooper (1984)	$h = 55P_r^{0.12-0.4343\ln(R_p)}(-0.4343\ln P_r)M^{-0.5}\left(\frac{q}{A}\right)^{0.67}$ (6) where h is in W/(m²·K), q/A is in W/m², and R_p is surface roughness in μm
	Gorenflo (1993)	$h = h_oF_{PF}\left(\frac{q/A}{(q/A)_o}\right)^{nf}\left(\frac{R_p}{R_{po}}\right)^{0.133}$ (7) where reference conditions are $(q/A)_o$ = 6300 Btu/h·ft², R_{po} = 0.4 μm $F_{PF} = 1.2P_r^{0.27} + 2.5P_r + \frac{P_r}{1-P_r}$ (8) $nf = 0.9 - 0.3P_r^{0.3}$ (9) For all fluids except water and helium.

Fluid	h_o, Btu/h·ft²·°F
R-134a	790
R-22	690
Ammonia	1230

Critical heat flux	Kutateladze (1951) Zuber et al. (1962)	$\frac{q/A}{\rho_v h_{fg}}\left[\frac{\rho^2 v}{\sigma_t g(\rho_l-\rho_v)}\right]^{0.25} = K_D$ (10) For many liquids, K_D varies from 0.12 to 0.16. Recommended average value is 0.13.
Minimum heat flux in film boiling from horizontal plate	Zuber (1959)	$\frac{q/A}{\rho_v h_{fg}}\left[\frac{(\rho_l+\rho_v)}{\sigma_t g(\rho_l-\rho_v)}\right]^{0.25} = 0.09$ (11)
Minimum heat flux in film boiling from horizontal cylinders	Lienhard and Wong (1963)	$\frac{q/A}{\rho_v h_{fg}}\left[\frac{(\rho_l+\rho_v)^2}{\sigma_t g(\rho_l-\rho_v)}\right]^{0.25} = 0.114\frac{\left[\frac{2\sigma_t}{g(\rho_l-\rho_v)D^2}\right]^{0.5}}{\left[1+\frac{2\sigma_t}{g(\rho_l-\rho_v)D^2}\right]^{0.25}}$ (12)
Minimum temperature difference for film boiling from horizontal plate	Berenson (1961)	$(t_w - t_{sat}) = 0.127\frac{\rho_v h_{fg}}{k_v}\left[\frac{g(\rho_l-\rho_v)}{\rho_l+\rho_v}\right]^{2/3} \times\left[\frac{\sigma_t}{g(\rho_l-\rho_v)}\right]^{0.5}\left[\frac{\mu_v}{\rho_l-\rho_v}\right]^{1/3}$ (13)
Film boiling from horizontal plate	Berenson (1961)	$h = 0.425\left[\frac{k_v^3\rho_v h_{fg}g(\rho_l-\rho_v)}{\mu_v(t_w-t_{sat})\sqrt{\phi_t/g(\rho_l-\rho_v)}}\right]^{0.25}$ (14)
Film boiling from horizontal cylinders	Anderson et al. (1966)	$h = 0.62\left[\frac{k_v^3\rho_v g(\rho_l-\rho_v)h_{fg}}{D\mu_v(t_w-t_{sat})}\right]^{0.25}$ (15)
Effect of radiation	Anderson et al. (1966)	Substitute $h'_{fg} = h_{fg}\left[1+0.4c_p\frac{t_w-t_b}{h_{fg}}\right]$

Table 1 Equations for Boiling Heat Transfer (*Continued*)

Description	References	Equations	
Effect of surface tension and of pipe diameter	Breen and Westwater (1962)	$\Lambda/D < 0.8$: $h(\Lambda)^{0.25}/F = 0.60$	(16)
		$0.8 < \Lambda/D < 8$: $hD^{0.25}/F = 0.62$	(17)
		$8 < \Lambda/D$: $h(\Lambda)^{0.25}/F = 0.016\,(\Lambda/D)^{0.83}$	(18)
		where $\Lambda = 2\pi\left[\frac{\sigma_t}{g(\rho_l - \rho_v)}\right]^{0.25}$	
		$F = \left[\frac{\rho_v h_{fg} g(\rho_l - \rho_v) k_v^3}{\mu_v (t_w - t_{sat})}\right]^{0.25}$	
Turbulent film	Frederking and Clark (1962)	$\mathrm{Nu} = 0.15\,(\mathrm{Ra})^{1/3}$ for $\mathrm{Ra} > 5 \times 10^7$	(19)
		$\mathrm{Ra} = \left[\frac{D^3 g(\rho_l - \rho_v)}{\nu_v^2 \rho_v}\left(\frac{c_p \mu}{k}\right)_v \left(\frac{h_{fg}}{c_p(t_w - t_{sat})} + 0.4\right)\frac{a}{g}\right]^{1/3}$	
		a = local acceleration	

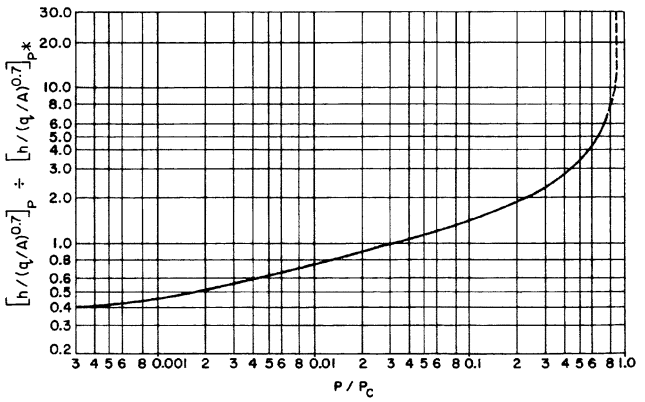

Fig. 3 Correlation of Pool Boiling Data in Terms of Reduced Pressure

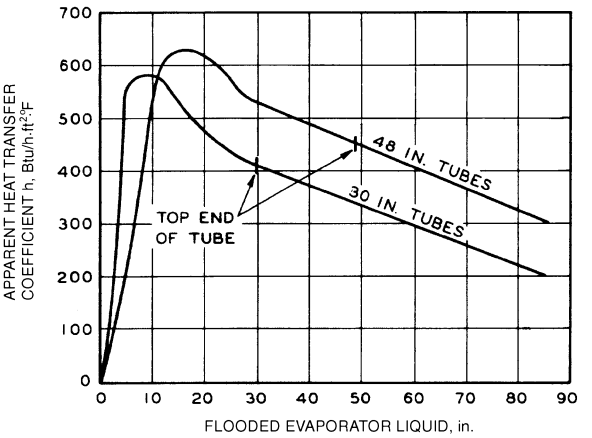

Fig. 4 Boiling Heat Transfer Coefficients for Flooded Evaporator

Maximum Heat Flux and Film Boiling

Maximum or critical heat flux and the film boiling region are not as strongly affected by conditions of the heating surface as the heat flux in the nucleate boiling region, making analysis of DNB and of film boiling more tractable.

Carey (1992) provides a review of the mechanisms that have been postulated to cause the DNB phenomenon in pool boiling. Each model is based on the scenario that vapor blankets, which lead to an increased thermal resistance, exist on portions of the heat transfer surface. It has been proposed that these blankets may result from Helmholtz instabilities.

When DNB (point *a*, Figure 1) is assumed to be a hydrodynamic instability phenomenon, a simple relation, Equation (10) in Table 1, can be derived to predict this flux for pure, wetting liquids (Kutateladze 1951, Zuber et al. 1962). The dimensionless constant K varies from approximately 0.12 to 0.16 for a large variety of liquids. The effect of wettability is still in question. Van Stralen (1959) found that for liquid mixtures, DNB is a function of the concentration.

The minimum heat flux density (point *b*, Figure 1) in film boiling from a horizontal surface and a horizontal cylinder can be predicted by Equations (11) and (12) in Table 1. The numerical factors 0.09 and 0.114 were adjusted to fit experimental data; values predicted by two analyses were approximately 30% higher. Equation (13) in Table 1 predicts the temperature difference at minimum heat flux of film boiling.

The heat transfer coefficient in film boiling from a horizontal surface can be predicted by Equation (14) in Table 1; and from a horizontal cylinder by Equation (15) in Table 1 (Bromley 1950), which has been generalized to include the effect of surface tension and cylinder diameter, as shown in Equations (16), (17), and (18) in Table 1 (Breen and Westwater 1962).

Frederking and Clark (1962) found that for turbulent film boiling, Equation (19) in Table 1 agrees with data from experiments at reduced gravity (Rohsenow 1963, Westwater 1963, Kutateladze 1963, Jakob 1949 and 1957).

Flooded Evaporators

Equations in Table 1 merely approximate heat transfer rates in flooded evaporators. One reason is that vapor entering the evaporator combined with vapor generated within the evaporator can produce significant forced convection effects superimposed on those caused by nucleation. Nonuniform distribution of the two-phase, vapor-liquid flow within the tube bundle of shell-and-tube evaporators or the tubes of vertical-tube flooded evaporators is also important.

Bundle data and design methods for plain, low fin, and enhanced tubes have been reviewed in Thome (1990) and Collier and Thome (1996).

Typical performance of vertical tube natural circulation evaporators, based on data for water, is shown in Figure 4 (Perry 1950). Low coefficients are at low liquid levels because insufficient liquid covers the heating surface. The lower coefficient at high levels is the result of an adverse effect of hydrostatic head on temperature difference and circulation rate. Perry (1950) noted similar effects in horizontal shell-and-tube evaporators.

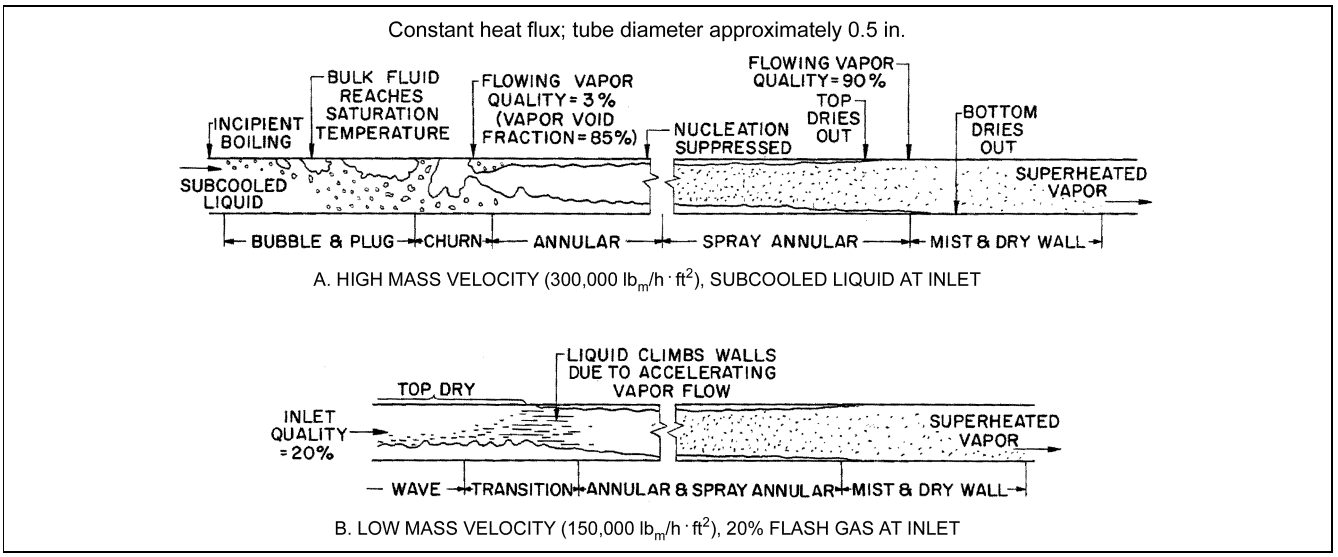

Fig. 5 Flow Regimes in Typical Smooth Horizontal Tube Evaporator

Forced-Convection Evaporation in Tubes

Flow Mechanics. When a mixture of liquid and vapor flows inside a tube, a number of flow patterns occur, depending on the mass fraction of liquid, the fluid properties of each phase, and the flow rate. In an evaporator tube, the mass fraction of liquid decreases along the circuit length, resulting in a series of changing vapor-liquid flow patterns. If the fluid enters as a subcooled liquid, the first indications of vapor generation are bubbles forming at the heated tube wall (nucleation). Subsequently, bubble, plug, churn (or semiannular), annular, spray annular, and mist flows can occur as the vapor content increases for two-phase flows in horizontal tubes. Idealized flow patterns are illustrated in Figure 5A for a horizontal tube evaporator.

Because nucleation occurs at the heated surface in a thin sublayer of superheated liquid, boiling in forced convection may begin while the bulk of the liquid is subcooled. Depending on the nature of the fluid and the amount of subcooling, the bubbles formed can either collapse or continue to grow and coalesce (Figure 5A), as Gouse and Coumou (1965) observed for R-113. Bergles and Rohsenow (1964) developed a method to determine the point of incipient surface boiling.

After nucleation begins, bubbles quickly agglomerate to form vapor plugs at the center of a vertical tube, or, as shown in Figure 5A, vapor plugs form along the top surface of a horizontal tube. At the point where the bulk of the fluid reaches saturation temperature, which corresponds to local static pressure, there will be up to 1% vapor quality because of the preceding surface boiling (Guerrieri and Talty 1956).

Further coalescence of vapor bubbles and plugs results in churn, or semiannular flow. If the fluid velocity is high enough, a continuous vapor core surrounded by a liquid annulus at the tube wall soon forms. This annular flow occurs when the ratio of the tube cross section filled with vapor to the total cross section is approximately 85%. With common refrigerants, this equals a vapor quality of about 0% to 30%. **Vapor quality** is the ratio of mass (or mass flow rate) of vapor to total mass (or mass flow rate) of the mixture. The usual flowing vapor quality or vapor fraction is referred to throughout this discussion. Static vapor quality is smaller because the vapor in the core flows at a higher average velocity than the liquid at the walls (see Chapter 2).

If two-phase mass velocity is high (greater than 150,000 $lb_m/h \cdot ft^2$ for a 0.5 in. tube), annular flow with small drops of entrained liquid in the vapor core (spray) can persist over a vapor quality range from about 10% to more than 90%. Refrigerant evaporators are fed from an expansion device at vapor qualities of approximately 20%, so that annular and spray annular flow predominate in most tube lengths. In a vertical tube, the liquid annulus is distributed uniformly over the periphery, but it is somewhat asymmetric in a horizontal tube (Figure 5A). As vapor quality reaches about 80%, the surface dries out. Chaddock and Noerager (1966) found that in a horizontal tube, dryout occurs first at the top of the tube and progresses toward the bottom with increasing vapor quality (Figure 5A).

If two-phase mass velocity is low (less than 150,000 $lb_m/h \cdot ft^2$ for a 0.5 in. horizontal tube), liquid occupies only the lower cross section of the tube. This causes a wavy type of flow at vapor qualities above about 5%. As the vapor accelerates with increasing evaporation, the interface is disturbed sufficiently to develop annular flow (Figure 5B). Liquid slugging can be superimposed on the flow configurations illustrated; the liquid forms a continuous, or nearly continuous, sheet over the tube cross section. The slugs move rapidly and at irregular intervals. Kattan et al. (1998a) presented a general method for prediction of flow pattern transitions (i.e., a flow pattern map) based on observations for R-134a, R-125, R-502, R-402A, R-404A, R-407C, and ammonia.

Heat Transfer. It is difficult to develop a single relation to describe the heat transfer performance for evaporation in a tube over the full quality range. For refrigerant evaporators with several percentage points of flash gas at entrance, it is less difficult because annular flow occurs in most of the tube length. The reported data are accurate only within geometry, flow, and refrigerant conditions tested; therefore, a large number of methods for calculating heat transfer coefficients for evaporation in tubes is presented in Table 2 (also see Figures 6 through 8).

Figure 6 gives heat transfer data for R-22 evaporating in a 0.772 in. tube (Gouse and Coumou 1965). At low mass velocities (below 150,000 $lb_m/h \cdot ft^2$), the wavy flow regime shown in Figure 5B probably exists, and the heat transfer coefficient is nearly constant along the tube length, dropping at the tube exit as complete vaporization occurs. At higher mass velocities, the flow pattern is usually annular, and the coefficient increases as vapor accelerates. As the surface dries and the flow reaches a 90% vapor quality, the coefficient drops sharply.

Equation (1) in Table 2 is used to estimate average heat transfer coefficients for refrigerants evaporating in horizontal tubes (Pierre

Table 2 Equations for Forced Convection Evaporation in Tubes

Equations		Comments and References
Horizontal Tubes		
$h = C_1\left(\frac{k_l}{d}\right)\left[\left(\frac{GD}{\mu_l}\right)^2\left(\frac{J\Delta x h_{fg}}{L}\right)\right]^n$	(1)	Average coefficients for R-12 and R-22 evaporating in copper tubes of 0.472 and 0.709 in. ID, from 13.4 to 31.2 ft long, and at evaporating temperatures from –4 to 32°F (Pierre 1955, 1957).
where $C_1 = 0.0009$ and $n = 0.5$ for exit qualities < 90% $C_1 = 0.0082$ and $n = 0.4$ for 11°F superheat at exit		
Equation (1) with $C_1 = 0.0225$ and $n = 0.375$		Average coefficients for R-22 evaporating at temperatures from 40 to 80°F in a 0.343 in. ID tube, 8 ft long (Altman et al. 1960b).
$h = Eh_f + Sh_{ncb}$ *where*	(2)	Compiled from a data base of 3693 data points including data for R-11, R-12, R-22, R-113, R-114, and water. Useful for vertical flows and horizontal flows (Gungor and Winterton 1986).
$E = 1 + 24{,}000B_o^{1.16} + 1.37(1/X_{tt})^{0.86}$	(3)	
$S = [1 + 0.00000115E^2\mathrm{Re}_l^{1.17}]^{-1}$	(4)	
$h_f = 0.023\mathrm{Re}_l^{0.8}\mathrm{Pr}_l^{0.4}(k_l/d)$	(5)	
$\mathrm{Re}_l = \frac{G(1-x)d}{\mu_l}$	(6)	
h_{ncb} is found from Equation (6) in Table 1, which has units W/m^2. If tube is horizontal and Fr < 0.05, use following multipliers: $E_2 = \mathrm{Fr}_L^{(0.1-2\mathrm{Fr}_l)}$ $S_2 = \mathrm{Fr}_l^{1/2}$		
$h = (C_1C_o^{C_2}(25\mathrm{Fr}_L) + C_3B_o^{C_4}F_{fl})h_f$	(7)	Compiled from a database of 5246 data points including data for R-11, R-12, R-22, R-113, R-114, R-152a, nitrogen, neon, and water. Tube sizes ranged from 0.25 in. to 1.25 in. (Kandlikar 1990).

where h_f is found from Equations (5) and (6) shown above.

Constant	Convective	Nucleate Boiling
C_1	1.136	0.6683
C_2	–0.9	–0.2
C_3	667.2	1058
C_4	0.7	0.7
C_5	0.3	0.3

Use convective constants if $C_o < 0.65$ and nucleate if $C_o > 0.65$. $C_5 = 0$ for vertical tubes and horizontal with $\mathrm{Fr}_l > 0.04$.

Fluid	F_{fl}
R-22	2.2
R-12	1.5
R-152a	1.1

Vertical Tubes		
$h = 3.4h_l(1/X_{tt})^{0.45}$	(8)	Equations (8) and (9) were fitted to experimental data for vertical upflow in tubes. Both relate to forced-convection evaporation regions where nucleate boiling is suppressed (Guerrieri and Talty 1956, Dengler and Addoms 1956). A multiplying factor is recommended when nucleation is present.
$h = 3.5h_L(1/X_{tt})^{0.5}$	(9)	
where h_l is from (3), X_{tt} from (7), h_L from (6)		
$h = 0.74h_L[B_o \times 10^4 + (1/X_{tt})^{0.67}]$	(10)	Local coefficients for water in vertical upflow in tubes with diameters from 0.1162 to 0.4317 in. and lengths of 15 to 40 in. The boiling number B_o accounts for nucleation effects, and the Martinelli parameter X_{tt}, for forced-convection effects (Schrock and Grossman 1962).
where B_o is from (5), h_L from (6), X_{tt} from (7)		
$h = h_{mic} + h_{mac}$	(11)	Chen developed this correlation reasoning that the nucleation transfer mechanism (represented by h_{mic}) and the convective transfer mechanism (represented by h_{mac}) are additive. h_{mac} is expressed as a function of the two-phase Reynolds number after Martinelli, and h_{mic} is obtained from the nucleate boiling correlation of Forster and Zuber (1955). S_c is a suppression factor for nucleate boiling (Chen 1963).
where $h_{mac} = h_lF_c$	(12)	
$h_{mic} = 0.00122\,(S_c)(E)(\Delta t)^{0.24}(\Delta p)^{0.75}$	(13)	
F_c and S_c from Figures 7 and 8		
$E = \frac{k_l^{0.79}(c_p)_l^{0.45}\rho_l^{0.49}g_c^{0.25}}{\sigma_t^{0.50}\mu_l^{0.29}h_{fg}^{0.24}\rho_v^{0.24}}$		

Note: Except for dimensionless equations, units are lb_m, h, ft, °F, and Btu.

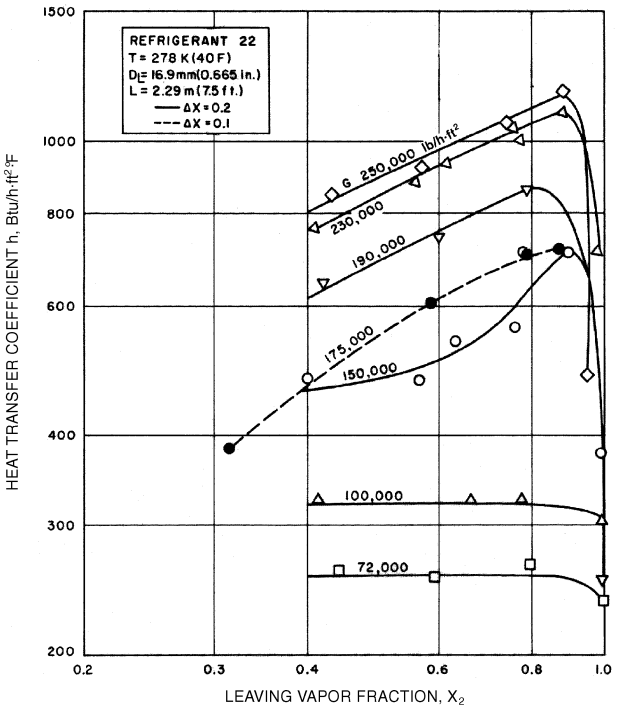

Fig. 6 Heat Transfer Coefficient Versus Vapor Fraction for Partial Evaporation

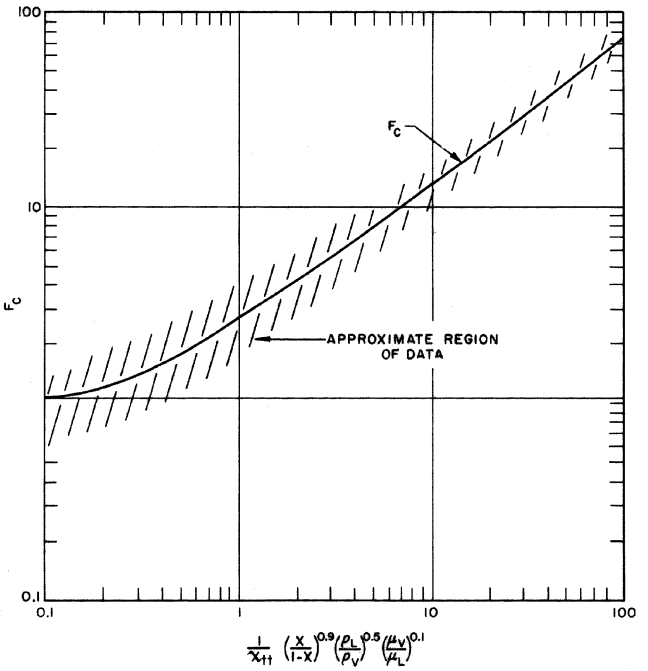

Fig. 7 Reynolds Number Factor F_c

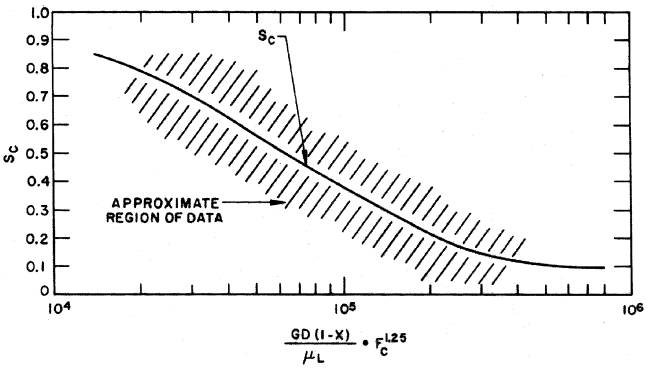

Fig. 8 Suppression Factor S_c

1955, 1957). A number of methods are also available to estimate local heat transfer coefficients during evaporation. Equations (2) through (6) in Table 2 summarize the Gungor and Winterton (1986) model, while Equation (7) gives the Kandlikar (1990) model. In addition, the Shah (1982) model is also recommended for estimating local heat transfer coefficients during annular flow. These local models have been found accurate for a wide range of refrigerants but do not include mechanisms to model dryout. The flow pattern based model of Kattan et al. (1998b) includes specific models for each flow pattern type and has been tested with the newer refrigerants such as R-134a and R-407C.

Heat transfer coefficients during flow in vertical tubes can be estimated with Equations (8), (9), and (10) in Table 2. The Chen correlation shown in Equations (11) through (13) in Table 2 includes terms for the velocity effect (convection) and heat flux (nucleation) and produces local heat transfer coefficients as a function of local vapor quality. The method developed by Steiner and Taborek (1992) includes an asymptotic model for the convection and nucleation component of heat transfer and is recommended for most situations.

The effect of lubricant on the evaporation heat transfer coefficients has been studied by a number of authors (Schalger et al. 1988, Eckels et al. 1993, and Zeurcher et al. 1999). Schalger et al. and Eckels et al. showed that the average heat transfer coefficients during evaporation of R-22 and R-134a in smooth and enhanced tubes are in general decreased by presence of lubricant (up to a 20% reduction at a 5% lubricant concentration by mass). Slight enhancements at lubricant concentrations under 3% are observed with some refrigerant lubricant mixtures. Zeurcher et al. (1999) studied local heat transfer coefficients of refrigerant/lubricant mixtures in the dry wall region of the evaporator (see Figure 5) and proposed prediction methods. The effect of lubricant concentration on local heat transfer coefficients was shown to be dependent on the mass flux and vapor quality. At low mass fluxes, the oil sharply decreased performance, while at higher mass fluxes, enhancements at certain vapor qualities were seen.

CONDENSING

In most applications that use the condensation process, condensation is initiated by removing heat at a solid-vapor interface, either through the walls of the vessel containing the saturated vapor or through the solid surface of a cooling mechanism placed within the saturated vapor. If a sufficient amount of energy is removed, the local temperature of the vapor near the interface will drop below its equilibrium saturation temperature. Because the heat removal process creates a temperature gradient with the lowest temperature near the interface, vapor droplets most likely form at this location. This defines one type of heterogeneous nucleation that can result in either dropwise condensation or film condensation, depending on the physical characteristics of the solid surface and the working fluid.

Dropwise condensation occurs on the cooling solid surface when its surface free energy is relatively low compared to that of the liquid. Examples of this type of interface include highly polished or fatty acid-impregnated surfaces in contact with steam. **Film condensation** occurs when a cooling surface having relatively high surface free energy contacts a fluid having lower surface free energy

(see Isrealachvili 1991). This is the type of condensation that occurs in most systems.

The rate of heat transport depends on the condensate film thickness, which depends on the rate of vapor condensation and the rate of condensate removal. At high reduced pressures, the heat transfer coefficients for dropwise condensation are higher than those available in the presence of film condensation at the same surface loading. At low reduced pressures, the reverse is true. For example, there is a reduction of 6 to 1 in the dropwise condensation coefficient of steam when saturation pressure is decreased from 0.9 to 0.16 atm. One method for correlating the dropwise condensation heat transfer coefficient employs nondimensional parameters, including the effect of surface tension gradient, temperature difference, and fluid properties.

When condensation occurs on horizontal tubes and short vertical plates, the condensate film motion is laminar. On vertical tubes and long vertical plates, the film motion can become turbulent. Grober et al. (1961) suggest using a Reynolds number (Re) of 1600 as the critical point at which the flow pattern changes from laminar to turbulent. This Reynolds number is based on condensate flow rate divided by the breadth of the condensing surface. For a vertical tube, the breadth is the circumference of the tube; for a horizontal tube, the breadth is twice the length of the tube. $Re = 4\Gamma/\mu_f$, where Γ is the mass flow of condensate per unit of breadth, and μ_f is the absolute (dynamic) viscosity of the condensate at the film temperature t_f. In practice, condensation is usually laminar in shell-and-tube condensers with the vapor outside horizontal tubes.

Vapor velocity also affects the condensing coefficient. When this is small, condensate flows primarily by gravity and is resisted by the viscosity of the liquid. When vapor velocity is high relative to the condensate film, there is appreciable drag at the vapor-liquid interface. The thickness of the condensate film, and hence the heat transfer coefficient, is affected. When vapor flow is upward, a retarding force is added to the viscous shear, increasing the film thickness. When vapor flow is downward, the film thickness decreases and the heat transfer coefficient increases. For condensation inside horizontal tubes, the force of the vapor velocity causes

Table 3 Heat Transfer Coefficients for Film-Type Condensation

Description	References	Equations	
1. **Vertical surfaces**, height L			
Laminar condensate flow, $Re = 4\Gamma/\mu_f < 1800$	McAdams (1954)	$h = 1.13F_1(h_{fg}/L\Delta t)^{0.25}$	(1)
	McAdams (1954)	$h = 1.11F_2(b/w_l)^{1/3}$	(2)
	Grigull (1952)	$h = 0.003(F_1)^2(\Delta tL/\mu_f^2 h_{fg})^{0.5}$	(3)
Turbulent flow, $Re = 4\Gamma/\mu_f > 1800$	McAdams (1954)	$h = 0.0077F_2(\mathrm{Re})^{0.4}(1/\mu_f)^{1/3}$	(4)
2. **Outside horizontal tubes**, N rows in a vertical plane, length L, laminar flow			
	McAdams (1954)	$h = 0.79F_1(h_{fg}/Nd\Delta t)^{0.25}$	(5)
	McAdams (1954)	$h = 1.05F_2(L/w_l)^{1/3}$	(6)
Finned tubes	Beatty and Katz (1948)	$h = 0.689F_1(h_{fg}/\Delta tD_e)^{0.25}$ where D_e is determined from $\frac{1}{(D_e)^{0.25}} = 1.30\frac{A_s\phi}{A_{eff}(L_{mf})^{0.25}} + \frac{A_p}{A_{eff}(D)^{0.25}}$ with $A_{eff} = A_s\phi + A_p$ and $L_{mf} = a_f/D_o$	(7)
3. **Simplified equations for steam**			
Outside vertical tubes, $Re = 4\Gamma/\mu_f < 2100$	McAdams (1954)	$h = 4000/(L)^{0.25}(\Delta t)^{1/3}$	(8)
Outside horizontal tubes, $Re = 4\Gamma/\mu_f < 1800$	McAdams (1954)		
Single tube		$h = 3100/(d')^{0.25}(\Delta t)^{1/3}$	(9a)
Multiple tubes		$h = 3100/(Nd')^{0.25}(\Delta t)^{1/3}$	(9b)
4. **Inside vertical tubes**	Carpenter and Colburn (1949)	$h = 0.065\left(\frac{c_{pf}k_f\rho_f f'}{2\mu_f\rho_v}\right)^{0.5} G_m$ where $G_m = \left(\frac{G_i^2 + G_iG_o + G_o^2}{3}\right)^{0.5}$	(10)
5. **Inside horizontal tubes**, $\frac{DG_l}{\mu_l} < 5000$			
$1000 < \frac{DG_v}{\mu_l}\left(\frac{\rho_l}{\rho_v}\right)^{0.5} < 20{,}000$	Ackers and Rosson (1960)	$\frac{hD}{k_l} = 13.8\left(\frac{c_p\mu_l}{k_l}\right)^{1/3}\left(\frac{h_{fg}}{c_p\Delta t}\right)^{1/6}\left[\frac{DG_v}{\mu_l}\left(\frac{\rho_l}{\rho_v}\right)^{0.5}\right]^{0.2}$	(11)
$20{,}000 < \frac{DG_v}{\mu_l}\left(\frac{\rho_l}{\rho_v}\right)^{0.5} < 100{,}000$	Ackers and Rosson (1960)	$\frac{hD}{k_l} = 0.1\left(\frac{c_p\mu_l}{k_l}\right)^{1/3}\left(\frac{h_{fg}}{c_p\Delta t}\right)^{1/6}\left[\frac{DG_v}{\mu_l}\left(\frac{\rho_l}{\rho_v}\right)^{0.5}\right]^{2/3}$	(12)
For $\frac{DG_l}{\mu_l} > 5000$ $\frac{DG_v}{\mu_l}\left(\frac{\rho_l}{\rho_v}\right)^{0.5} > 20{,}000$	Ackers et al. (1959)	$\frac{hD}{k_l} = 0.026\left(\frac{c_p\mu_l}{k_l}\right)^{1/3}\left(\frac{DG_e}{\mu_l}\right)^{0.8}$ where $G_e = G_v(\rho_l/\rho_v)^{0.5} + G_l$	(13)

Notes: 1. Equations (1) through (10) are dimensional with units of Btu, h, ft, °F, and lb_m. 2. t_f = liquid film temperature = $t_{sat} - 0.75\Delta t$

the condensate to flow. When the vapor velocity is high, the transition from laminar to turbulent flow occurs at Reynolds numbers lower than previously described [i.e., 1600 according to Grober et al. (1961)].

When **superheated** vapor is condensed, the heat transfer coefficient depends on the surface temperature. When the surface temperature is *below* saturation temperature, using the value of h for condensation of saturated vapor that incorporates the difference between the *saturation* temperature and the surface temperature leads to insignificant error (McAdams 1954). If the surface temperature is *above* the saturation temperature, there is no condensation and the equations for gas convection apply.

Correlation equations for condensing heat transfer are given in Table 3. Factors F_1 and F_2, which depend only on the physical properties of the working fluid and which occur often in these equations, have been computed for some commonly used refrigerants in Table 4. Refrigerant properties used in the calculations may be found in Chapter 19.

In some cases, the equations are given in two forms: one is convenient when the amount of refrigerant to be condensed or the condensing load is known; the second is useful when the difference between the vapor temperature and the condensing surface temperature is known.

Condensation on Outside Surface of Vertical Tubes

For film-type condensation on the outside surface of vertical tubes and on vertical surfaces, Equations (1) and (2) in Table 3 are recommended when $4\Gamma/\mu_f$ is less than 1800 (McAdams 1954). For these equations, fluid properties are evaluated at the mean film temperature. When $4\Gamma/\mu_f$ is greater than 1800 (tall vertical plates or tubes), use Equation (3) or (4) in Table 3. Equations (2) and (4) in Table 3 are plotted in Figure 9. The theoretical curve for laminar film-type condensation is shown for comparison. A semitheoretical relationship for turbulent film-type condensation is also shown for Pr values of 1.0 and 5.0 (Colburn 1933-34).

Condensation on Outside Surface of Horizontal Tubes

For a bank of N tubes, Nusselt's equations, increased by 10% (Jakob 1949 and 1957), are given in Equations (5) and (6) in Table 3. Experiments by Short and Brown (1951) with R-11 suggest that drops of condensation falling from row to row cause local turbulence and increase heat transfer.

For condensation on the outside surface of horizontal finned tubes, Equation (7) in Table 3 is used for liquids that drain readily from the surface (Beatty and Katz 1948). For condensing steam outside finned tubes, where liquid is retained in the spaces between the tubes, coefficients substantially lower than those given by Equation (7) in Table 3 were reported. For additional data on condensation outside finned tubes, see Katz et al. (1947). For more on this topic, refer to Webb (1994).

Table 4 Values of Condensing Coefficient Factors for Different Refrigerants (from Chapter 19)

Refrigerant	Film Temperature, °F $t_f = t_{sat} - 0.75\Delta t$	F_1	F_2
Refrigerant 11	75	154	822
	100	153	815
	125	151	803
Refrigerant 12	75	133	672
	100	122	608
	125	112	538
Refrigerant 22	75	153	822
	100	144	755
	125	132	675
Sulfur Dioxide	75	290	1920
	100	299	2000
	125	318	2170
Ammonia	75	409	3040
	100	408	3035
	125	408	3030
Propane	75	159	850
	100	157	845
	125	154	836
Butane	75	156	840
	100	156	843
	125	157	845

$$F_1 = \left(\frac{k_f^3 \rho_f^2 g}{\mu_f}\right)^{0.25} \qquad \text{Units: } \left[\frac{(\text{Btu})^3(\text{lb}_\text{m})}{(\text{h})^4(\text{ft})^7(°\text{F})^3}\right]^{0.25}$$

$$F_2 = \left(\frac{k_f^3 \rho_f^2 g}{\mu_f}\right)^{1/3} \qquad \text{Units: } \left[\frac{(\text{Btu})^3(\text{lb}_\text{m})}{(\text{h})^4(\text{ft})^7(°\text{F})^3}\right]^{1/3}$$

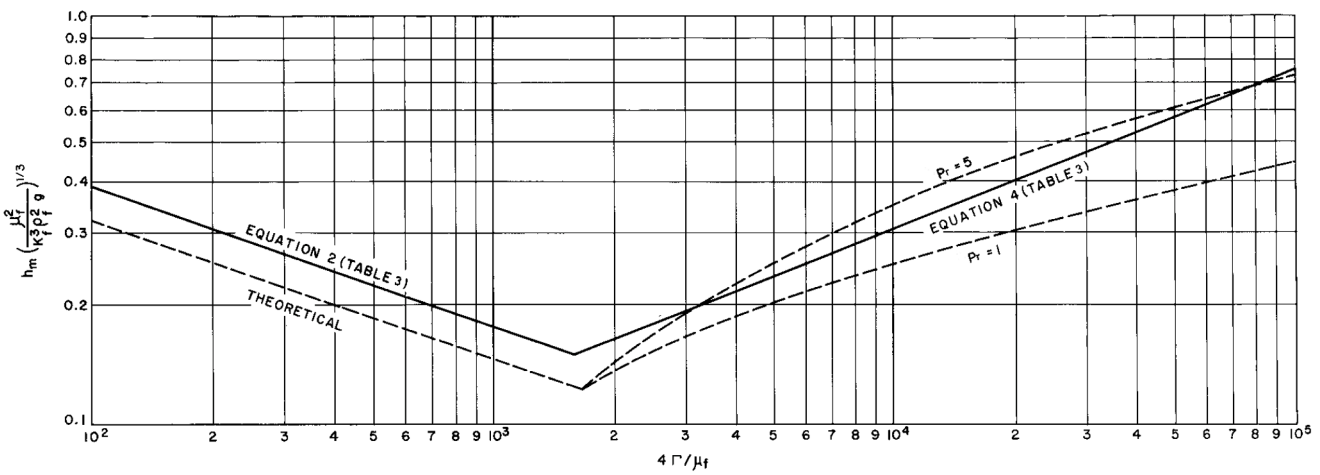

Fig. 9 Film-Type Condensation

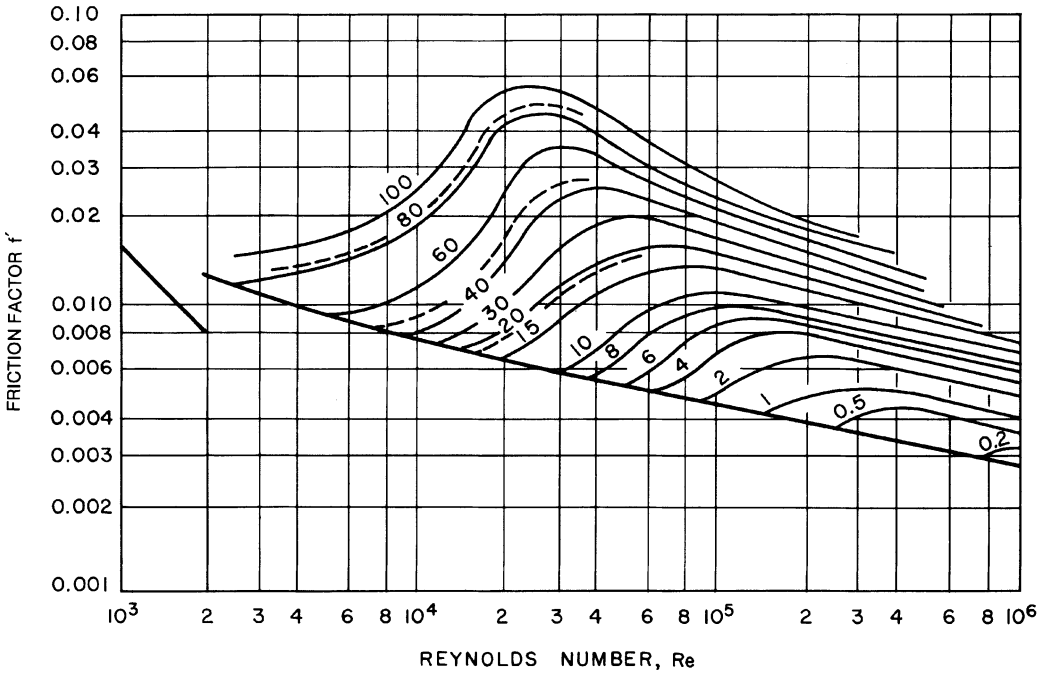

Curve parameter = $\Gamma/\rho s$, where Γ = liquid flow rate, ρ = liquid density, and s = surface tension of liquid relative to water; values of gas velocity used in calculating f and Re are calculated as though no liquid were present.

Fig. 10 Friction Factors for Gas Flow Inside Pipes with Wetted Walls

Simplified Equations for Steam

For film-type steam condensation at atmospheric pressure and film temperature drops of 10 to 150°F, McAdams (1954) recommends Equations (8) and (9) in Table 3.

Condensation on Inside Surface of Vertical Tubes

Condensation on the inside surface of tubes is generally affected by appreciable vapor velocity. The measured heat transfer coefficients are as much as 10 times those predicted by Equation (4) in Table 3. For vertical tubes, Jakob (1949 and 1957) gives theoretical derivations for upward and downward vapor flow. For downward vapor flow, Carpenter and Colburn (1949) suggest Equation (10) in Table 3. The friction factor f' for vapor in a pipe containing condensate should be taken from Figure 10.

Condensation on Inside Surface of Horizontal Tubes

For condensation on the inside surface of horizontal tubes (as in air-cooled condensers, evaporative condensers, and some shell-and-tube condensers), the vapor velocity and resulting shear at the vapor-liquid interface are major factors in analyzing heat transfer. Hoogendoorn (1959) identified seven types of two-phase flow patterns. For semistratified and laminar annular flow, use Equations (11) and (12) in Table 3 (Ackers and Rosson 1960). Ackers et al. (1959) recommend Equation (13) in Table 3 for turbulent annular flow (vapor Reynolds number greater than 20,000 and liquid Reynolds number greater than 5000). For high mass flux (> 40 lb/s·ft^2), the method of Shah (1979) is recommended for predicting local heat transfer coefficients during condensation. A method for using a flow regime map to predict the heat transfer coefficient for condensation of pure components in a horizontal tube is presented in Breber et al. (1980). More recently, the flow regime dependent method of Dobson and Chato (1998) provides a more accurate design approach.

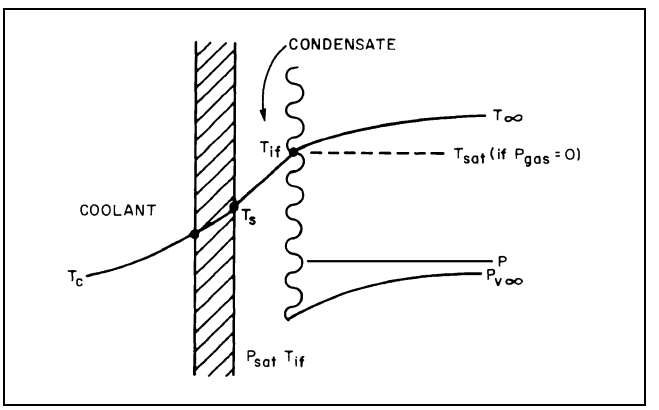

Fig. 11 Origin of Noncondensable Resistance

Noncondensable Gases

Condensation heat transfer rates reduce drastically if one or more noncondensable gases are present in the condensing vapor/gas mixture. In mixtures, the condensable component is termed **vapor** and the noncondensable component is called **gas**. As the mass fraction of gas increases, the heat transfer coefficient decreases in an approximately linear manner. In a steam chest with 2.89% air by volume, Othmer (1929) found that the heat transfer coefficient dropped from about 2000 to about 600 Btu/h·ft^2·°F. Consider a surface cooled to some temperature t_s below the saturation temperature of the vapor (Figure 11). In this system, accumulated condensate falls or is driven across the condenser surface. At a finite heat transfer rate, a temperature profile develops across the condensate that can be estimated from Table 3; the interface of the condensate is at a temperature $t_{if} > t_s$. In the absence of gas, the interface temperature is the vapor saturation temperature at the pressure of the condenser.

The presence of noncondensable gas lowers the vapor partial pressure and hence the saturation temperature of the vapor in equilibrium with the condensate. Further, the movement of the vapor toward the cooled surface implies similar bulk motion of the gas. At the condensing interface, the vapor is condensed at temperature t_{if} and is then swept out of the system as a liquid. The gas concentration rises to ultimately diffuse away from the cooled surface at the same rate as it is convected toward the surface (Figure 11). If gas (mole fraction) concentration is Y_g and total pressure of the system is p, the partial pressure of the bulk gas is

$$p_{g\infty} = Y_{g\infty} p \tag{2}$$

The partial pressure of the bulk vapor is

$$p_{v\infty} = (1 - Y_{g\infty})p = Y_{v\infty} p \tag{3}$$

As opposing fluxes of convection and diffusion of the gas increase, the partial pressure of gas at the condensing interface is $p_{gif} > p_{g\infty}$. By Dalton's law, assuming isobaric condition,

$$p_{gif} + p_{vif} = p \tag{4}$$

Hence, $p_{vif} < p_{v\infty}$.

Sparrow et al. (1967) noted that thermodynamic equilibrium exists at the interface, except in the case of very low pressures or liquid metal condensation, so that

$$p_{vif} = p_{sat}(t_{if}) \tag{5}$$

where $p_{sat}(t)$ is the saturation pressure of the vapor at temperature t. The available Δt for condensation across the condensate film is reduced from $(t_\infty - t_s)$ to $(t_{if} - t_s)$, where t_∞ is the bulk temperature of the condensing vapor-gas mixture, caused by the additional noncondensable resistance.

The equations in Table 3 are still valid for the condensate resistance, but the interface temperature t_{if} must be found. The noncondensable resistance, which accounts for the temperature difference $(t_\infty - t_{if})$, depends on the heat flux (through the convecting flow to the interface) and the diffusion of gas away from the interface.

In simple cases, Sparrow et al. (1967), Rose (1969), and Sparrow and Lin (1964) found solutions to the combined energy, diffusion, and momentum problem of noncondensables, but they are cumbersome.

A general method given by Colburn and Hougen (1934) can be used over a wide range if correct expressions are provided for the rate equations—add the contributions of the sensible heat transport through the noncondensable gas film and the latent heat transport via condensation:

$$h_g(t_\infty - t_{if}) + K_D M_v h_{lv}(p_{v\infty} - p_{vif}) = h(t_{if} - t_s) = U(t_{if} - t_c) \tag{6}$$

where h is from the appropriate equation in Table 3.

The value of the heat transfer coefficient for the stagnant gas depends on the geometry and flow conditions. For flow parallel to a condenser tube, for example,

$$j = \left(\frac{h_g}{(c_p)_g G}\right)\left(\frac{(c_p)_g \mu_{gv}}{K_{Dg}}\right)^{2/3} \tag{7}$$

where j is a known function of $\mathrm{Re} = GD/\mu_{gv}$.

The mass transfer coefficient K_D is

$$\frac{K_D}{M_m}\left[\frac{p_{g\infty} - p_{gif}}{\ln(p_{g\infty}/p_{gif})}\right]\left(\frac{\mu_{gv}}{\rho_g D}\right)^{2/3} = j \tag{8}$$

The calculation method requires substitution of Equation (8) into Equation (6). For a given flow condition, G, Re, j, M_m, $p_{g\infty}$, h_g, and h (or U) are known. Assume values of t_{if}; calculate $p_{sat}(t_{if}) = p_{vif}$ and hence p_{gif}. If t_s is not known, use the overall coefficient U to the coolant and t_c in place of h and t_s in Equation (6). For either case, at each location in the condenser, iterate Equation (6) until it balances, giving the condensing interface temperature and, hence, the thermal load to that point (Colburn and Hougen 1934, Colburn 1951). For more detail, refer to Chapter 10 in Collier and Thome (1996).

Other Impurities

Vapor entering the condenser often contains a small percentage of impurities such as oil. Oil forms a film on the condensing surfaces, creating additional resistance to heat transfer. Some allowance should be made for this, especially in the absence of an oil separator or when the discharge line from the compressor to the condenser is short.

PRESSURE DROP

Total pressure drop for two-phase flow in tubes consists of friction, acceleration, and gravitational components. It is necessary to know the **void fraction** (the ratio of gas flow area to total flow area) to compute the acceleration and gravitational components. To compute the frictional component of pressure drop, either the **two-phase friction factor** or the **two-phase frictional multiplier** must be determined.

The homogeneous model provides a simple method for computing the acceleration and gravitational components of pressure drop. The homogeneous model assumes that the flow can be characterized by average fluid properties and that the velocities of the liquid and vapor phases are equal (Collier and Thome 1996, Wallis 1969).

Martinelli and Nelson (1948) developed a method for predicting the void fraction and two-phase frictional multiplier to use with a separated flow model. This method predicts the pressure drops of boiling refrigerants reasonably well. Other methods of computing the void fraction and two-phase frictional multiplier used in a separated flow model are given in (Collier and Thome 1996, Wallis 1969).

The general nature of annular gas-liquid flow in vertical, and to some extent horizontal, pipe is indicated in Figure 12 (Wallis 1970), which plots the effective gas friction factor versus the liquid fraction $(1 - a)$. Here a is the void fraction, or fraction of the pipe cross section taken up by the gas or vapor.

The effective gas friction factor is defined as

$$f_{eff} = \left[\frac{a^{5/2} D}{2\rho_g (4Q_g/\pi D^2)^2}\right]\left(-\frac{dp}{ds}\right) \tag{9}$$

where D is the pipe diameter, ρ_g the gas density, and Q_g the gas volumetric flow rate. The friction factor of gas flowing by itself in the pipe (presumed smooth) is denoted by f_g. Wallis' analysis of the flow occurrences is based on interfacial friction between the gas and liquid. The wavy film corresponds to a conduit of relative roughness ε/D, about four times the liquid film thickness. Thus, the pressure drop relation of vertical flow is

$$-\frac{dp}{ds} + \rho_g g = 0.01\left(\frac{\rho_g}{D^5}\right)\left(\frac{4Q_g}{\pi}\right)^2 \frac{1 + 75(1-a)}{a^{5/2}} \tag{10}$$

This corresponds to the Martinelli-type analysis with

$$f_{two\text{-}phase} = \phi_g^2 f_g$$

when

$$\phi_g^2 = \frac{1 + 75(1-a)}{a^{5/2}} \tag{11}$$

The friction factor f_g (of the gas alone) is taken as 0.02, an appropriate turbulent flow value. This calculation can be modified for more detailed consideration of factors such as Reynolds number variation in friction, gas compressibility, and entrainment (Wallis 1970).

In two-phase flow inside horizontal tubes, the pressure gradient is written as the sum of frictional and momentum terms. Thus,

$$\frac{dp}{dz} = \left(\frac{dp}{dz}\right)_f + \left(\frac{dp}{dz}\right)_m \tag{12}$$

In adiabatic two-phase flow, the contribution of the momentum transfer to the overall pressure drop is negligibly small; theoretically, it is nonexistent if the flow is fully developed. In condensation heat transfer, the momentum transfer term contributes to the overall pressure drop due to the mass transfer that occurs at the liquid-vapor interface.

Two basic models were used in developing frictional pressure drop correlations for two-phase adiabatic flow. In the first, the flow of both phases is assumed to be homogeneous; the gas and liquid velocities are assumed equal. The frictional pressure drop is computed as if the flow were single phase, except for introducing modifiers to the single-phase friction coefficient. In the second model, the two phases are considered separate, and the velocities may differ. Two correlations used to predict the frictional pressure drop are those of Lockhart and Martinelli (1949) and Dukler et al. (1964).

In the Lockhart-Martinelli correlation, a parameter X was defined as

$$X = \left[\left(\frac{dp}{dz}\right)_l \div \left(\frac{dp}{dz}\right)_v \right]^{0.5} \tag{13}$$

where

$\left(\frac{dp}{dz}\right)_l$ = frictional pressure gradient, assuming that liquid alone flows in pipe

$\left(\frac{dp}{dz}\right)_v$ = frictional pressure gradient, assuming that gas (or vapor in case of condensation) alone flows in pipe

The frictional pressure gradient due to the single-phase flow of the liquid or vapor depends on the type of flow of each phase, laminar or turbulent. For turbulent flow during condensation, replace X by X_{tt}. Thus,

$$X_{tt} = \left(\frac{1-x}{x}\right)^{0.9} \left(\frac{\mu_l}{\mu_v}\right)^{0.1} \left(\frac{\rho_v}{\rho_l}\right)^{0.5} \tag{14}$$

Lockhart and Martinelli (1949) also defined ϕ_v as

$$\phi_v = \left[\left(\frac{dp}{dz}\right)_f \div \left(\frac{dp}{dz}\right)_v \right]^{0.5} \tag{15}$$

For condensation,

$$\left(\frac{dp}{dz}\right)_v = -\frac{2f_o(xG)^2}{\rho_v D_i} \tag{16}$$

where

$$f_o = \frac{0.045}{(GxD_i/\mu_v)^{0.2}} \tag{17}$$

Here f_o is the friction factor for adiabatic two-phase flow.

By analyzing the pressure drop data of simultaneous adiabatic flow of air and various liquids, Lockhart and Martinelli (1949) correlated the parameters ϕ_v and X and reported the results graphically. Soliman et al. (1968) approximated the graphical results of ϕ_v versus X_{tt} by

$$\phi_v = 1 + 2.85X_{tt}^{0.523} \tag{18}$$

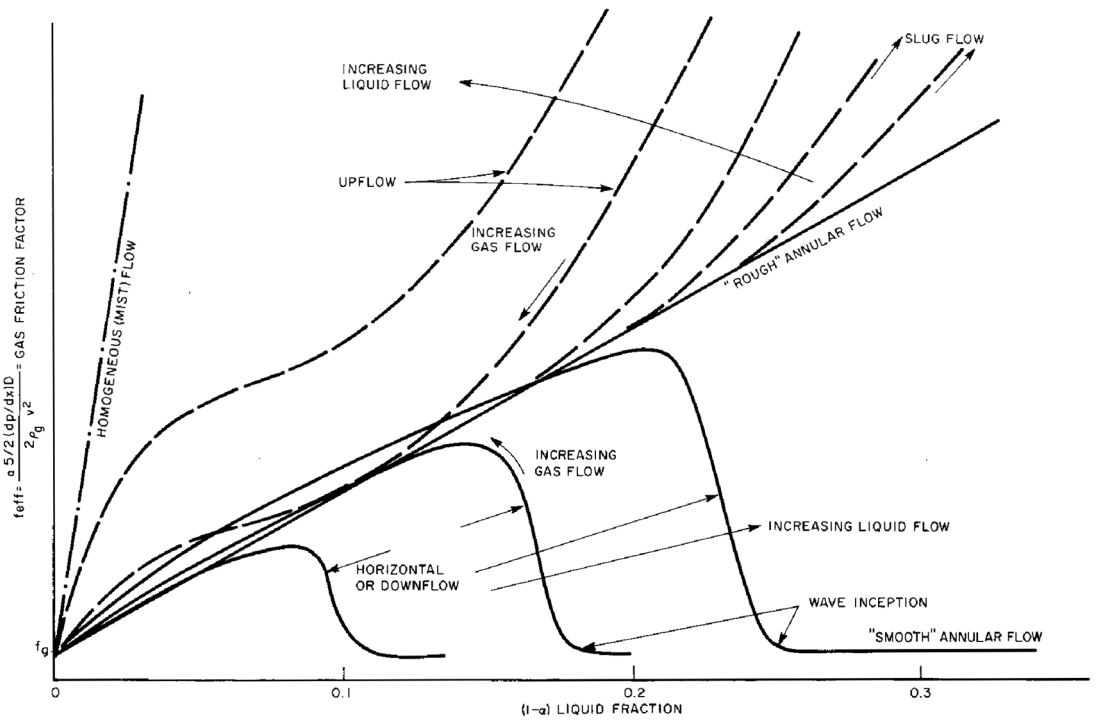

Fig. 12 Qualitative Pressure Drop Characteristics of Two-Phase Flow Regime

In the correlation of Dukler et al. (1964), the frictional pressure gradient is given by

$$\left(\frac{dp}{dz}\right)_f = -\frac{2G^2 f_o \alpha(\lambda)\beta}{D_i \rho_{NS}} \tag{19}$$

where

f_o = single-phase friction coefficient evaluated at two-phase Reynolds number

$$= 0.0014 + 0.125\left(\frac{4\dot{m}_l\beta}{\pi D_i \mu_{NS}}\right)^{-0.32} \tag{20}$$

$$\alpha(\lambda) = 1 - (\ln\lambda)/[1.281 + 0.478\ln\lambda + 0.444(\ln\lambda)^2 + 0.094(\ln\lambda)^3 + 0.00843(\ln\lambda)^4] \tag{21}$$

$$\beta = \left(\frac{\rho_l}{\rho_{NS}}\right)\frac{\lambda^2}{(1-\psi)} + \left(\frac{\rho_v}{\rho_{NS}}\right)\frac{(1-\lambda)^2}{\psi} \tag{22}$$

$$\rho_{NS} = \rho_l\lambda + \rho_v(1-\lambda) \tag{23}$$

$$\mu_{NS} = \mu_l\lambda + \mu_v(1-\lambda) \tag{24}$$

$$\lambda = 1/\left(1 + \frac{x}{(1-x)}\frac{\rho_v}{\rho_e}\right) \tag{25}$$

Because the correlations mentioned here were originally developed for adiabatic two-phase flow, Luu and Bergles (1980) modified the friction coefficients in Equations (16) and (19), using the modifier suggested by Silver and Wallis (1965-66). The modification replaced the friction coefficient f_o with the friction coefficient f_{co}. These terms are related by

$$\left(\frac{f_{co}}{f_o}\right) = \exp\left(\frac{\varepsilon}{2f_o}\right) - \left(\frac{\xi}{f_o}\right) \tag{26}$$

where

$$\xi = \left(\frac{D_i\psi}{2x}\right)\frac{dx}{dz} \tag{27}$$

Because the Lockhart-Martinelli and Dukler correlations for the frictional pressure gradient were based on the separated flow model, the momentum pressure gradient should be as well. Thus,

$$\left(\frac{dp}{dz}\right)_m = -G^2\left(\frac{dx}{dz}\right)\left\{\frac{2x}{\rho_v\psi} - \frac{2(1-x)}{\rho_l(1-\psi)} + q_l\left[\frac{\psi 1-x}{x1-\psi\rho_l} - \frac{x(1-\psi)}{\psi(1-x)\rho_v}\right]\right\} \tag{28}$$

To determine $(dp/dz)_m$, the void fraction ψ and the quality gradient must be known. A generalized expression for ψ was suggested by Butterworth (1975):

$$\psi = \frac{1}{1 + A_l[(1-x)/x]^{q_l}(\rho_v/\rho_l)^{r_l}(\mu_l/\mu_v)^{S_l}} \tag{29}$$

Table 5 Constants in Equation (29) for Different Void Fraction Correlations

Model	A_l	q_l	r_l	S_l
Homogeneous (Collier 1972)	1.0	1.0	1.0	0
Lockhart-Martinelli (1949)	0.28	0.64	0.36	0.07
Baroczy (1963)	1.0	0.74	0.65	0.13
Thom (1964)	1.0	1.0	0.89	0.18
Zivi (1964)	1.0	1.0	0.67	0
Turner-Wallis (1965)	1.0	0.72	0.40	0.08

where A_l, q_l, r_l, and S_l are constants and are listed for the various correlations in Table 5.

The quality gradient dx/dz in Equation (28) can be estimated by assuming a constant rate of cooling. In the case of complete condensation, its value is $-1/L$, where L is the length of the condenser tube.

Evaporators and condensers often have valves, tees, bends, and other fittings that contribute to the overall pressure drop of the heat exchanger. Collier and Thome (1996) summarize methods predicting the two-phase pressure drop in these fittings.

ENHANCED SURFACES

Enhanced heat transfer surfaces are used in heat exchangers to improve performance and decrease cost. Condensing heat transfer is often enhanced with circular fins attached to the external surfaces of tubes to increase the heat transfer area. Other enhancement methods, such as porous coatings, integral fins, and reentrant cavities, are used to augment boiling heat transfer on the external surfaces of evaporator tubes. Webb (1981) surveys external boiling surfaces and compares the performances of several enhanced surfaces with the performance of smooth tubes. For heat exchangers, the heat transfer coefficient for the refrigerant side is often smaller than the coefficient for the water side. Thus, enhancing the refrigerant-side surface can reduce the size of the heat exchanger and improve its performance.

Internal fins increase the heat transfer coefficients during evaporation or condensation in tubes. However, internal fins increase the refrigerant pressure drop and reduce the heat transfer rate by decreasing the available temperature difference between hot and cold fluids. Designers should carefully determine the number of parallel refrigerant passes that give optimum loading for best overall heat transfer.

For additional information on enhancement methods in two-phase flow, consult Bergles (1976, 1985), Thome (1990), and Webb (1994).

SYMBOLS

A = area
A_{eff} = total effective area [Equation (7) in Table 3]
a = local acceleration [Equation (19) in Table 1]; void fraction [Equations (9) and (10)]
a_f = area of one side of one film
B_o = boiling number [Equations (3) and (7) in Table 2]
b = breadth of a condensing surface. For vertical tube, $b = \pi d$; for horizontal tube, $b = 2L$
C = a coefficient or constant
C_o = convection number
$C_1 \ldots C_5$ = special constants (see Table 2)
c_p = specific heat at constant pressure
c_v = specific heat at constant volume
D = diameter
D_d = bubble departure diameter [Equation (5) in Table 1]
D_i = inside tube diameter
D_o = outside tube diameter
d = diameter; or prefix meaning differential
(dp/dz) = pressure gradient

$(dp/dz)_f$ = frictional pressure gradient
$(dp/dz)_l$ = frictional pressure gradient, assuming that liquid alone is flowing in pipe
$(dp/dz)_m$ = momentum pressure gradient
$(dp/dz)_v$ = frictional pressure gradient, assuming that gas (or vapor) alone is flowing in pipe
E = special coefficient (Table 2)
F_c = Reynolds number factor [Equation (12) in Table 2 and Figure 7]
F_{PF} = special coefficient [Equation (7) in Table 1]
Fr = Froude number
F_1, F_2 = condensing coefficient factors (Table 4)
f = friction factor for single-phase flow
f' = friction factor for gas flow inside pipes with wetted walls (Figure 10)
f_{co} = friction factor in presence of condensation [Equation (26)]
f_o = friction factor [Equations (17) and (19)]
G = mass velocity
Gr = Grashof number
g = gravitational acceleration
g_c = gravitational constant
h = heat transfer coefficient
h_f = special coefficient [Equation (7) in Table 1]
h_{fg} = latent heat of vaporization or of condensation
j = Colburn j-factor
K_D = mass transfer coefficient
k = thermal conductivity
L = length
L_{mf} = mean length of fin [Equation (7) in Table 3]
ln = natural logarithm
M = mass; or molecular weight
M_m = mean molecular weight of vapor-gas mixture
M_v = molecular weight of condensing vapor
m = general exponent [Equations (1) and (6) in Table 1]
$\dot{m}$ = mass rate of flow
N = number of tubes in vertical tier
Nu = Nusselt number
n = general exponent [Equations (1) and (6) in Table 1]
Pr = Prandtl number
p = pressure
p_c = critical thermodynamic pressure for coolant
p_r = reduced pressure
Q = total heat transfer
q = rate of heat transfer
r = radius
Ra = Rayleigh number
Re = Reynolds number
R_p = surface roughness, μm
S = distance along flow direction
S_c = suppression factor (Table 2 and Figure 8)
t = temperature
U = overall heat transfer coefficient
V = linear velocity
x = quality (i.e., vapor fraction = M_v/M); or distance in dt/dx
X_{tt} = Martinelli parameter [Figure 7, Table 2, and Equation (14)]
x,y,z = lengths along principal coordinate axes
Y_g = mole fraction of gas [Equations (2) and (3)]
Y_v = mole fraction of vapor [Equation (3)]
α = thermal diffusivity = $k/\rho c_p$
α(λ) = ratio of two-phase friction factor to single-phase friction factor at two-phase Reynolds number [Equation (21)]
β = ratio of two-phase density to no-slip density [Equation (22)]
Γ = mass rate of flow of condensate per unit of breadth (see section on Condensing)
Δ = difference between values
ε = roughness of interface
Λ = special coefficient [Equations (16) through (19) in Table 1]
λ = ratio of liquid volumetric flow rate to total volumetric flow rate [Equation (25)]
μ = absolute (dynamic) viscosity
μ_l = dynamic viscosity of saturated liquid
μ_{NS} = dynamic viscosity of two-phase homogeneous mixture [Equation (24)]
μ_v = dynamic viscosity of saturated vapor
ν = kinematic viscosity
ρ = density
ρ_l = density of saturated liquid
ρ_{NS} = density of two-phase homogeneous mixture [Equation (23)]
ρ_v = density of saturated vapor phase
σ = surface tension
ϕ_g = fin efficiency, Martinelli factor [Equation (11)]
ϕ_v = Lockhart-Martinelli parameter [Equation (15)]
ψ = void fraction

Subscripts and Superscripts

a = exponent in Equation (1)
b = bubble
c = critical or cold (fluid)
cg = condensing
e = equivalent
eff = effective
f = film or fin
g = gas
h = horizontal or hot (fluid) or hydraulic
i = inlet or inside
if = interface
L = liquid
l = liquid
m = mean
mac = convective mechanism [Equations (11) through (13) in Table 2]
max = maximum
mic = nucleation mechanism [Equations (11) through (13) in Table 2]
min = minimum
ncb = nucleate boiling
o = outside or outlet or overall
r = root (fin) or reduced pressure
s = surface or secondary heat transfer surface
sat = saturation (pressure)
t = temperature or terminal temperature of tip (fin)
v = vapor or vertical
w = wall
∞ = bulk
* = reference

REFERENCES

Ackers, W.W., H.A. Deans, and O.K. Crosser. 1959. Condensing heat transfer within horizontal tubes. *Chemical Engineering Progress Symposium Series* 55(29):171-76.

Ackers, W.W. and H.F. Rosson. 1960. Condensation inside a horizontal tube. *Chemical Engineering Progress Symposium Series* 56(30):145-50.

Altman, M., F.W. Staub, and R.H. Norris. 1960b. Local heat transfer and pressure drop for Refrigerant-22 condensing to horizontal tubes. *Chemical Engineering Progress Symposium Series* 56(30):151-60.

Anderson, W., D.G. Rich, and D.F. Geary. 1966. Evaporation of Refrigerant 22 in a horizontal 3/4-in. OD tube. *ASHRAE Transactions* 72(1):28.

Baroczy, C.J. 1963. Correlation of liquid fraction in two-phase flow with application to liquid metals. *North American Aviation Report* SR-8171, El Segundo, CA.

Beatty, K.O. and D.L. Katz. 1948. Condensation of vapors on outside of finned tubes. *Chemical Engineering Progress* 44(1):55.

Berenson, P.J. 1961. Film boiling heat transfer from a horizontal surface. *ASME Journal of Heat Transfer* 85:351.

Berenson, P.J. 1962. Experiments on pool boiling heat transfer. *International Journal of Heat and Mass Transfer* 5:985.

Bergles, A.E. 1976. Survey and augmentation of two-phase heat transfer. *ASHRAE Transactions* 82(1):891-905.

Bergles, A.E. 1985. Techniques to augment heat transfer. In *Handbook of heat transfer application*, 2nd ed. McGraw-Hill, New York.

Bergles, A.E. and W.M. Rohsenow. 1964. The determination of forced convection surface-boiling heat transfer. *ASME Journal of Heat Transfer*, Series C, 86(August):365.

Borishansky, W. and A. Kosyrev. 1966. Generalization of experimental data for the heat transfer coefficient in nucleate boiling. *ASHRAE Journal* (May):74.

Borishansky, V.M., I.I. Novikov, and S.S. Kutateladze. 1962. Use of thermodynamic similarity in generalizing experimental data on heat transfer. Proceedings of the International Heat Transfer Conference.

Breber, G., J.W. Palen, and J. Taborek. 1980. Prediction of the horizontal tubeside condensation of pure components using flow regime criteria. *ASME Journal of Heat Transfer* 102(3):471-76.

Breen, B.P. and J.W. Westwater. 1962. Effects of diameter of horizontal tubes on film boiling heat transfer. AIChE Preprint No. 19, Fifth National Heat Transfer Conference, Houston, TX. *Chemical Engineering Progress* 58(7):67-72.

Bromley, L.A. 1950. Heat transfer in stable film boiling. *Chemical Engineering Progress* (46):221.

Butterworth, D. 1975. A comparison of some void-fraction relationships for co-current gas-liquid flow. *International Journal of Multiphase Flow* 1:845-50.

Carey, V.P. 1992. *Liquid-vapor phase change phenomena: An introduction to the thermophysics of vaporization and condensation processes in heat transfer equipment*. Hemisphere Publishing Corporation, Washington, D.C.

Carpenter, E.F. and A.P. Colburn. 1949. The effect of vapor velocity on condensation inside tubes. General discussion on Heat Transfer and Fluid Mechanics Institute, American Society of Mechanical Engineers, New York.

Chaddock, J.B. and J.A. Noerager. 1966. Evaporation of Refrigerant 12 in a horizontal tube with constant wall heat flux. *ASHRAE Transactions* 72(1):90.

Chen, J.C. 1963. A correlation for boiling heat transfer to saturated fluids on convective flow. ASME *Paper* 63-HT-34. American Society of Mechanical Engineers, New York.

Colburn, A.P. 1933-34. Note on the calculation of condensation when a portion of the condensate layer is in turbulent motion. *AIChE Transactions* No. 30.

Colburn, A.P. 1951. Problems in design and research on condensers of vapours and vapour mixtures. Proceedings of the Institute of Mechanical Engineers, 164:448, London.

Colburn, A.P. and O.A. Hougen. 1934. Design of cooler condensers for mixtures of vapors with noncondensing gases. *Industrial and Engineering Chemistry* 26 (November):1178.

Collier, J.G. and J.R. Thome. 1996. *Convective boiling and condensation*, 3rd ed. Oxford University Press.

Cooper, M.G. 1984. Heat flow rates in saturated nucleate pool boiling-a wide-ranging examination using reduced properties. *Advances in Heat Transfer.* Academic Press, Orlando, 16, 157-239.

Danilova, G. 1965. Influence of pressure and temperature on heat exchange in the boiling of halogenated hydrocarbons. *Kholodilnaya Teknika*, No. 2. English abstract, *Modern Refrigeration* (December).

Dengler, C.E. and J.N. Addoms. 1956. Heat transfer mechanism for vaporization of water in a vertical tube. *Chemical Engineering Progress Symposium Series* 52(18):95.

Dobson, M.K., and J.C. Chato. 1998. Condensation in smooth horizontal tubes. *Journal of Heat Transfer* 120:193-213.

Dougherty, R.L. and H.J. Sauer, Jr. 1974. Nucleate pool boiling of refrigerant-oil mixtures from tubes. *ASHRAE Transactions* 80(2):175.

Dukler, A.E., M. Wicks, III, and R.G. Cleveland. 1964. Frictional pressure drop in two-phase flow: An approach through similarity analysis. *AIChE Journal* 10(January):44-51.

Eckels, S.J., T.M. Doer, and M.B. Pate. 1994. In-tube heat transfer and pressure drop of R-134a and ester lubricant mixtures in a smooth tube and a micro-fin tube: Part 1 evaporation. *ASHRAE Transactions* 100(2)(1994): 265-82.

Farber, E.A. and R.L. Scorah. 1948. Heat transfer to water boiling under pressure. ASME *Transactions* (May):373.

Forster, H.K. and N. Zuber. 1955. Dynamics of vapor bubbles and boiling heat transfer. *AIChE Journal* 1(4):531-35.

Frederking, T.H.K. and J.A. Clark. 1962. Natural convection film boiling on a sphere. In *Advances in cryogenic engineering*, ed. K.D. Timmerhouse, Plenum Press, New York.

Furse, F.G. 1965. Heat transfer to Refrigerants 11 and 12 boiling over a horizontal copper surface. *ASHRAE Transactions* 71(1):231.

Gorenflo, D. 1993. Pool boiling. *VDI-Heat Atlas*. VDI-Verlag, Düsseldorf.

Gouse, S.W., Jr. and K.G. Coumou. 1965. Heat transfer and fluid flow inside a horizontal tube evaporator, Phase I. *ASHRAE Transactions* 71(2):152.

Green, G.H. and F.G. Furse. 1963. Effect of oil on heat transfer from a horizontal tube to boiling Refrigerant 12-oil mixtures. *ASHRAE Journal* (October):63.

Grigull, U. 1952. Wärmeübergang bei Filmkondensation. *Forsch, Gebiete Ingenieurw.* 18.

Grober, H., S. Erk, and U. Grigull. 1961. *Fundamentals of heat transfer*. McGraw-Hill, New York.

Guerrieri, S.A. and R.D. Talty. 1956. A study of heat transfer to organic liquids in single tube boilers. *Chemical Engineering Progress Symposium Series* 52(18):69.

Gungor, K.E., and R.H.S. Winterton. 1986. A general correlation for flow boiling in tubes and annuli. *International Journal Heat Mass Transfer* 29:351-58.

Hoogendoorn, C.J. 1959. Gas-liquid flow in horizontal pipes. *Chemical Engineering Sciences* IX(1).

Hughmark, G.A. 1962. A statistical analysis of nucleate pool boiling data. *International Journal of Heat and Mass Transfer* 5:667.

Isrealachvili, J.N. 1991. *Intermolecular surface forces*. Academic Press, New York.

Jakob, M. 1949 and 1957. *Heat transfer*, Vols. I and II. John Wiley and Sons, New York.

Kandlikar, S.G. 1990. A general correlation for saturated two-phase flow and boiling heat transfer inside horizontal and vertical tubes. *Journal of Heat Transfer* 112:219-28.

Kattan, N., J.R. Thome, and D. Favrat. 1998a. Flow boiling in horizontal tubes Part 1: Development of diabatic two-phase flow pattern map. *Journal of Heat Transfer* 120(1):140-47.

Kattan, N., J.R. Thome, and D. Favrat. 1998b. Flow boiling in horizontal tubes Part 3: Development of new heat transfer model based on flow patterns. *Journal of Heat Transfer* 120(1):156-65.

Katz, D.L., P.E. Hope, S.C. Datsko, and D.B. Robinson. 1947. Condensation of Freon-12 with finned tubes. Part I, Single horizontal tubes; Part II, Multitube condensers. *Refrigerating Engineering* (March):211, (April): 315.

Kutateladze, S.S. 1951. A hydrodynamic theory of changes in the boiling process under free convection. Izvestia Akademii Nauk, USSR, *Otdelenie Tekhnicheski Nauk* 4:529.

Kutateladze, S.S. 1963. *Fundamentals of heat transfer.* E. Arnold Press, London.

Lienhard, J.H. and V.E. Schrock. 1963. The effect of pressure, geometry and the equation of state upon peak and minimum boiling heat flux. *ASME Journal of Heat Transfer* 85:261.

Lienhard, J.H. and P.T.Y. Wong. 1963. The dominant unstable wave length and minimum heat flux during film boiling on a horizontal cylinder. ASME *Paper* No. 63-HT-3. ASME-AIChE Heat Transfer Conference, Boston, August.

Lockhart, R.W. and R.C. Martinelli. 1949. Proposed correlation of data for isothermal two-phase, two-component flow in pipes. *Chemical Engineering Progress* 45(1):39-48.

Luu, M. and A.E. Bergles. 1980. Augmentation of in-tube condensation of R-113. ASHRAE *Research Project* RP-219.

Martinelli, R.C. and D.B. Nelson. 1948. Prediction of pressure drops during forced circulation boiling of water. *ASME Transactions* 70:695.

McAdams, W.H. 1954. *Heat transmission*, 3rd ed. McGraw-Hill, New York.

Nukiyama, S. 1934. The maximum and minimum values of heat transmitted from metal to boiling water under atmospheric pressure. *Journal of the Japanese Society of Mechanical Engineers* 37:367.

Othmer, D.F. 1929. The condensation of steam. *Industrial and Engineering Chemistry* 21(June):576.

Perry, J.H. 1950. *Chemical engineers handbook*, 3rd ed. McGraw-Hill, New York.

Pierre, B. 1955. S.F. Review. *A.B. Svenska Flaktafabriken*, Stockholm, Sweden 2(1):55.

Pierre, B. 1957. *Kylteknisk Tidskrift* 3 (May):129.

Pierre, B. 1964. Flow resistance with boiling refrigerant. *ASHRAE Journal* (September through October).

Rohsenow, W.M. 1963. Boiling heat transfer. In *Modern developments in heat transfer*, ed. W. Ibele. Academic Press, New York.

Rose, J.W. 1969. Condensation of a vapour in the presence of a noncondensable gas. *International Journal of Heat and Mass Transfer* 12:233.

Schlager, L.M., M.B. Pate, and A.E. Bergles. 1987. Evaporation and condensation of refrigerant-oil mixtures in a smooth tube and micro-fin tube. *ASHRAE Transactions* 93:293-316.

Schrock, V.E. and L.M. Grossman. 1962. Forced convection boiling in tubes. *Nuclear Science and Engineering* 12:474.

Shah, M.M. 1979. A general correlation for heat transfer during film condensation inside pipes. *International Journal Heat Mass Transfer* 22:547-56.

Shah, M.M. 1982. A new correlation for saturated boiling heat transfer: equations and further study. *ASHRAE Transactions* 88(1):185-96.

Short, B.E. and H.E. Brown. 1951. Condensation of vapors on vertical banks of horizontal tubes. American Society of Mechanical Engineers, New York.

Silver, R.S. and G.B. Wallis. 1965-66. A simple theory for longitudinal pressure drop in the presence of lateral condensation. Proceedings of Institute of Mechanical Engineering, 180 Part I(1):36-42.

Soliman, M., J.R. Schuster, and P.J. Berenson. 1968. A general heat transfer correlation for annular flow condensation. *Journal of Heat Transfer* 90:267-76.

Sparrow, E.M. and S.H. Lin. 1964. Condensation in the presence of a noncondensable gas. ASME *Transactions*, *Journal of Heat Transfer* 86C:430.

Sparrow, E.M., W.J. Minkowycz, and M. Saddy. 1967. Forced convection condensation in the presence of noncondensables and interfacial resistance. *International Journal of Heat and Mass Transfer* 10:1829.

Starczewski, J. 1965. Generalized design of evaporation heat transfer to nucleate boiling liquids. *British Chemical Engineering* (August).

Steiner, D., and J. Taborek. 1992. Flow boiling heat transfer in vertical tubes correlated by an asymptotic model. *Heat Transfer Engineering* 13(2), 43-69.

Stephan, K. 1963a. The computation of heat transfer to boiling refrigerants. *Kältetechnik* 15:231.

Stephan, K. 1963b. Influence of oil on heat transfer of boiling Freon-12 and Freon-22. Eleventh International Congress of Refrigeration, I.I.R. *Bulletin* No. 3.

Stephan, K. 1963c. A mechanism and picture of the processes involved in heat transfer during bubble evaporation. *Chemic. Ingenieur Technik* 35:775.

Stephan, K. and M. Abdelsalam. 1980. Heat transfer correlations for natural convection boiling. *International Journal of Heat and Mass Transfer* 23:73-87.

Thom, J.R.S. 1964. Prediction of pressure drop during forced circulation boiling water. *International Journal of Heat and Mass Transfer* 7:709-24.

Thome, J.R. 1990. *Enhanced boiling heat transfer*. Hemisphere (Taylor and Francis), New York.

Tschernobyiski, I. and G. Ratiani. 1955. *Kholodilnaya Teknika* 32.

Turner, J.M. and G.B. Wallis. 1965. The separate-cylinders model of two-phase flow. *Report* No. NYO-3114-6. Thayer's School of Engineering, Dartmouth College, Hanover, NH.

Van Stralen, S.J. 1959. Heat transfer to boiling binary liquid mixtures. *Chemical Engineering* (British) 4(January):78.

Wallis, G.B. 1969. *One-dimensional two-phase flow.* McGraw-Hill, New York.

Wallis, G.C. 1970. Annular two-phase flow, Part I: A simple theory, Part II: Additional effect. *ASME Transactions*, *Journal of Basic Engineering* 92D:59 and 73.

Webb, R.L. 1981. The evolution of enhanced surface geometrics for nucleate boiling. *Heat Transfer Engineering* 2(3-4):46-69.

Webb, J.R. 1994. *Enhanced boiling heat transfer.* John Wiley and Sons, New York.

Westwater, J.W. 1963. Things we don't know about boiling. In *Research in Heat Transfer*, ed. J. Clark. Pergamon Press, New York.

Worsoe-Schmidt, P. 1959. Some characteristics of flow-pattern and heat transfer of Freon-12 evaporating in horizontal tubes. *Ingenieren*, International edition, 3(3).

Zeurcher O., J.R. Thome, and D. Favrat. 1998. In-tube flow boiling of R-407C and R-407C/oil mixtures, part II: Plain tube results and predictions. *Int. J. HVAC&R Research* 4(4):373-399.

Zivi, S.M. 1964. Estimation of steady-state steam void-fraction by means of the principle of minimum entropy production. *Journal of Heat Transfer* 86:247-52.

Zuber, N. 1959. Hydrodynamic aspects of boiling heat transfer. U.S. Atomic Energy Commission, Technical Information Service, *Report* AECU 4439. Oak Ridge, TN.

Zuber, N., M. Tribus, and J.W. Westwater. 1962. The hydrodynamic crisis in pool boiling of saturated and subcooled liquids. Proceedings of the International Heat Transfer Conference 2:230, and discussion of the papers, Vol. 6.